fermentation

MDPI

Article

Monitoring *C. vulgaris* Cultivations Grown on Winery Wastewater Using Flow Cytometry

Teresa Lopes da Silva [1,*], Thiago Abrantes Silva [2], Bruna Thomazinho França [1], Belina Ribeiro [1] and Alberto Reis [1,*]

[1] Laboratório Nacional de Energia e Geologia, Unidade de Bioenergia e Biorefinarias, Estrada do Paço do Lumiar 22, 1649-038 Lisboa, Portugal; brunathomazinho@gmail.com (B.T.F.); belina.ribeiro@lneg.pt (B.R.)
[2] Department of Civil Engineering, Federal University of Viçosa (Universidade Federal de Vicosa/UFV), Av. Peter Henry Rolfs, s/n, Campus Universitario, Vicosa 36570-900, MG, Brazil; abrantes.t@gmail.com
* Correspondence: teresa.lopessilva@lneg.pt (T.L.d.S.); alberto.reis@lneg.pt (A.R.)

Abstract

Winery wastewater (WWW), if released untreated, poses a serious environmental threat due to its high organic load. In this study, *Chlorella vulgaris* was cultivated in diluted WWW to assess its suitability as a culture medium. Two outdoor cultivation systems—a 270 L raceway and a 40 L bubble column—were operated over 33 days using synthetic medium (control) and WWW. A flow cytometry (FC) protocol was implemented to monitor key physiological parameters in near-real time, including cell concentration, membrane integrity, chlorophyll content, cell size, and internal complexity. At the end of cultivation, the bubble column yielded the highest cell concentrations: 2.85×10^6 cells/mL (control) and 2.30×10^6 cells/mL (WWW), though with lower proportions of intact cells (25% and 31%, respectively). Raceway cultures showed lower cell concentrations: 1.64×10^6 (control) and 1.54×10^6 cells/mL (WWW), but higher membrane integrity (76% and 36% for control and WWW cultures, respectively). On average, cells grown in the bubble column had a 22% larger radius than those in the raceway, favouring sedimentation. Heterotrophic cells were more abundant in WWW cultures, due to the presence of organic carbon, indicating its potential for use as animal feed. This study demonstrates that FC is a powerful, real-time tool for monitoring microalgae physiology and optimising cultivation in complex effluents like WWW.

Keywords: winery wastewater; *C. vulgaris*; flow cytometry; SYTO9; propidium iodide; raceway; bubble column

Academic Editor: Alexander Dimitrov Kroumov

Received: 15 May 2025
Revised: 9 July 2025
Accepted: 16 July 2025
Published: 31 July 2025

Citation: Lopes da Silva, T.; Silva, T.A.; França, B.T.; Ribeiro, B.; Reis, A. Monitoring C. *vulgaris* Cultivations Grown on Winery Wastewater Using Flow Cytometry. *Fermentation* **2025**, *11*, 442. https://doi.org/10.3390/fermentation11080442

1. Introduction

Winery wastewater (WWW) usually results from several steps involved in wine production, such as water utilised to clean the tanks, grape cleaning and pressing transfer lines, floor washing, and wine losses [1].

WWW's organic load consists of sugars, organic acids, alcohols, and polyphenolic compounds [2]. The large liquid volumes generated (typically 0.5 to 14 L per L of wine produced) and high content of suspended solids have a negative impact on the environment if released without any treatment, since untreated WWW can pollute groundwater by changing its characteristics [3]. Moreover, during the vintage season, discharging WWW containing high chemical oxygen demand (COD) contents can affect WWW treatment systems, paralysing them. As a result, very strict limits have been legislated concerning the WWW parameters before their discharge into the environment [4].

WWW can be treated by physicochemical, biological, membrane, and advanced oxidation processes and combined technologies [4]. Among them, biological processes are the most suitable to treat WWW due to their high organic content [5]. Activated sludge is often used to treat WWW, removing the major contaminants, but the associated costs are high [6]. In addition, the resulting sludge poses environmental challenges due to its high organic load, low biodegradability, and potential phytotoxicity, which complicate disposal and limit its reuse [7]. Recent publications showed that the use of microalgae has been successful in the treatment of various types of agro-industrial wastewater, such as WWW [1,4,8], dairy wastewater [9], and lignocellulosic materials [10]. Ali et al. [11] stated that this approach can be effective and economical, as microalgae can grow on a variety of wastewaters, require relatively low energy inputs, and efficiently reduce nutrient and organic loads while generating minimal waste sludge. In addition, microalgae can efficiently remove heavy metals from wastewaters, resulting in a microalgal biomass contaminated, which requires further treatment [12]. This problem is not a major concern when using WWW, which typically contains low levels of such contaminants, and the resulting biomass may be suitable for feed or biofertilizer.

C. vulgaris is considered a robust and pollution-tolerant microalga and is thus appropriate to treat sewage sludge and wastewater of different types [13–15]. However, when grown on such effluents, *C. vulgaris* cells are exposed to potentially toxic compounds such as polyphenols, organic acids, and esters [8], which may compromise cell growth and thus the process productivity. Therefore, obtaining timely information on the physiological status of the culture will allow for adapting process parameters and improving yields. Traditional biomass monitoring methods—such as dry cell weight or ash-free dry weight—are time-consuming and do not provide early information, as results are available too late for in-process adjustments [16]. In contrast, flow cytometry (FC) enables rapid, at-line assessment of individual cell physiological characteristics, such as chlorophyll content, membrane integrity, cell size, and granularity [17]. These parameters offer deep insight into culture health and physiological dynamics. For bioreactor control, FC is particularly advantageous as it allows prompt detection of stress responses or population shifts, enabling timely interventions (e.g., nutrient adjustment, aeration, light management, etc.) before productivity declines. This is especially relevant when cultivating microalgae on variable and complex substrates like WWW, which contains inhibitory compounds that may affect cell physiology [18,19]. Importantly, industrial effluents usually contain microorganisms and particles that interfere with traditional biomass quantification [20,21]. FC overcomes this limitation by using chlorophyll autofluorescence and light scatter to distinguish *C. vulgaris* cells from debris, non-photosynthetic microorganisms, and background particles, thus enabling targeting microalgal populations, which allows accurate quantification of several cell parameters in complex matrices. Fluorescence–scatter gating strategies have been successfully validated for *C. vulgaris* in mixed cultures [22,23], while spectral "virtual filtering"—a computational technique used in spectral flow cytometry to isolate specific fluorescence signals—further enhances the discrimination of microalgal cells from non-cellular particles and background noise [24]. The present work reports a flow cytometric protocol for monitoring *C. vulgaris* cultivations grown on WWW. Different fluorescent dyes (SYTOX Green, carboxyfluorescein diacetate, SYTO9, propidium iodide) were previously tested to evaluate the microalgae cells' viability in terms of membrane integrity. The selected dyes were then used to monitor the cultures grown on a synthetic medium as a control assay, and on WWW, in a 750 L raceway and 100 L bubble column, for comparison of the impact of these systems on the microalgae cells, in terms of microbial population dynamics, chlorophyll production, cell size, and membrane integrity. The final microalgal biomass was further characterised in terms of protein and carbohydrate content for further potential applications.

2. Materials and Methods

2.1. Inoculum

Chlorella vulgaris inoculum was supplied by the company A4F (Póvoa de Santa Iria, Portugal), in a synthetic medium, with the following composition (g/L): KH_2PO_4 1.25; $NaHCO_3$ 0.50; KNO_3 1.25; $MgSO_47H_2O$ 1.00; $CaCl_2 \cdot 2H_2O$ 0.11; Fe-EDTA 0.012; 1 mL of trace element solution. The composition of the trace elements solution was as follows (g/L): H_3BO_3 2.860; $MnSO_4 \cdot 4H_2O$ 2.030; $ZnSO_4$ 0.220; $CoSO_4 \cdot 7H_2O$ 0.090; $CuSO_4$ 0.050.

2.2. Growth Media

WWW was kindly supplied by Adega Cooperativa de Palmela (winery producer, Palmela, Portugal) and was generated from the washing of equipment and other storage vessels in the cellar. Non-sterile WWW was diluted 1:1 with tap water since this dilution was found to provide the most favourable conditions for algal growth. Previous experiments showed that *C. vulgaris* grew poorly on pure WWW compared to the 1:1 dilution (unpublished data), likely due to the high organic load and the presence of inhibitory compounds present in the undiluted WWW. These experiments also demonstrated that the microalgal growth required nitrogen and phosphorous supplementation; otherwise, no growth occurred. In this way, 4.25 g/L of $NaNO_3$ and 0.34 g/L of KH_2PO_4 were added to the diluted WWW (WWW medium), which had the following original composition: 11,217.5 mg O_2/L COD, 4.00 mg/L total nitrogen, 6.49 mg/L nitrate, 23 mg/L total phosphate, 0.18 g/L lactic acid, and 4.27 g/L acetic acid. In all assays, before inoculation, the medium's pH was adjusted to 7.0 with NaOH. The synthetic medium was used as a control for the raceway and bubble column experiments.

2.3. Chlorella vulgaris Raceway Outdoor Cultivations

Two identical 750 L raceways of glass fibre (3 × 1 m, surface area/volume ratio = 11.1/m) were filled up to 270 L (corresponding to a liquid height of 10 cm), one with synthetic medium (control) and the other with WWW diluted 1:1 with tap water, supplemented with $NaNO_3$ and KH_2PO_4. Each raceway had two channels separated by a glass fibre island placed in the middle. Mixing was performed by paddle wheels placed at the end of the raceway, and each paddle wheel contained two blades, utilising natural light (Figure 1). The linear velocity was set to 30 cm/s (8.2 rpm). *Chlorella* inoculum (10% *v*/*v*) was added to both raceways at the same time. No air bubbling or CO_2 supply was provided. The microalgal cultures were cultivated under natural sunlight.

Figure 1. *Chlorella vulgaris* cultivations in raceways. Left side: raceway containing WWW; right side: raceway containing synthetic medium (control).

2.4. *Chlorella vulgaris* Bubble Column Outdoor Cultivations

For the bubble column trials, two identical acrylic cylinders 0.22 m in diameter and 1.78 m in height (100 L maximum) were used as bubble column photobioreactors, one containing 40 L of synthetic medium and the other containing 40 L of diluted (1:1) WWW, supplemented with $NaNO_3$ and KH_2PO_4, utilising sunlight. The columns were covered with an acrylic lid with a hole big enough to allow the tubes to pass through (Figure 2). The spargers, fixed to the bottom of each column, had a three-pointed star shape (10 cm in diameter), with a sprinkler at the end of each arm. Each sprinkler contained five evenly spaced holes (2.5 mm in diameter, 2 mm apart), designed to ensure uniform air distribution. Aeration was supplied at a rate of 0.2 vvm using a Resun LP-100 high-blow air pump (Resun, China). No air filter was used, as the cultivation was conducted under non-aseptic conditions. A 10% (*v*/*v*) *C. vulgaris* inoculum was added simultaneously to both bubble columns. The cultures were grown under natural sunlight.

Figure 2. *Chlorella vulgaris* cultivations in bubble columns. Left side: bubble column containing WWW; right side: bubble column containing synthetic medium (control).

2.5. FC Analysis

Samples taken throughout the microalgal cultivations in the raceways and bubble columns were analysed by FC for cell count, size, internal complexity and membrane integrity, using a flow cytometer (Beckman Coulter, CytoFLEX Flow Cytometer, Brea, CA, USA) equipped with two solid-state lasers, emitting at 488 and 638 nm, and two sensors for the detection of light scatter: forward (FSC) and side (SSC). FSC is proportional to cell size, while SSC is proportional to cell internal complexity. The equipment also includes six fluorescence detectors, FITC (525/40 bandpass (BP), PE (585/42 BP), PC5.5 (690/50), PC7 (789/60), and APC (660/10 BP), which detect intracellular fluorescent compounds, such as pigments or cells stained with specific fluorochromes for physiological status characterisation. The microalgae cells were identified based on their chlorophyll content. Since chlorophyll is a fluorescent compound that emits fluorescence between 600 nm and 700 nm, it was detected in the APC-A channel (660/10 BP). In this way, *C. vulgaris* populations could be discriminated from the background, and cells were counted by FC.

A few fluorescent dyes were previously tested to evaluate the physiological status of *C. vulgaris*. SYTOX Green (SYTOX, Invitrogen, Carlsbad, CA, USA) and carboxyfluorescein diacetate (CFDA, Invitrogen, Carlsbad, CA, USA) were used to evaluate the cell membrane integrity and enzymatic activity, respectively. SYTO9 and SYBR Green I (SYBR, Invitrogen, Carlsbad, CA, USA) fluorescent dyes were used in association with propidium iodide (PI) to evaluate the cell membrane integrity. SYTOX and PI dyes do not cross the plasma membranes of intact cells but easily penetrate cells with compromised membranes (permeabilized cells). In this way, it is possible to differentiate intact from permeabilized cells. CFDA is a hydrophobic molecule that enters intact cell membranes. Once inside the cell cytoplasm, CFDA is enzymatically hydrolysed by cellular esterases into carboxyfluorescein, which is a fluorescent and hydrophilic compound, thus revealing cells that have intact membranes and active esterases. SYBR Green I and SYTO9 enter all the cells, binding to DNA and increasing the cells' fluorescence, so they are used to differentiate cells from the background and are particularly helpful when cells are growing in media containing a high proportion of particles such as industrial effluents, including WWW. These dyes are usually used in association with PI for cell membrane integrity detection [25].

The dye concentrations and incubation times were previously optimised. Whenever necessary, samples were diluted in a phosphate-buffered solution (PBS) prepared using commercial tablets (pH 7.4; VWR International, LLC, Aurora, OH, USA) in a total volume of 500 µL, and incubated in the dark with 5 µL of SYTOX 30 µM solution for 25 min [SYTOX 30 µM solution was obtained by dilution of SYTOX 5 mM commercial solution (Invitrogen, Thermo Fisher Scientific, Carlsbad, CA, USA) in DMSO]. SYTOX is detected in the FITC-A channel when excited with radiation at 488 nm. A 3 µL amount of CFDA (Invitrogen by Thermo Fisher Scientific, Carlsbad, CA, USA) stock solution (10 mg/mL, diluted with acetone) was added to 500 µL of cell suspension, and incubated for 10 min in the dark, before FC analysis. CFDA is detected in the FITC-A channel when excited with radiation at 488 nm. For cells double-stained with SYBR and PI, 2 µL of SYBR solution [1:30 dilution of SYBR Green I commercial stock (from Invitrogen) solution made in dimethyl sulfoxide] and 2 µL of PI (Invitrogen by Thermo Fisher Scientific, Carlsbad, CA, USA) solution 1 mg/mL were added simultaneously to 500 µL of sample and incubated for 30 min in darkness. For cells double-stained with SYTO9 and PI, 3 µL of SYTO9 solution [1:50 dilution of 5 mM commercial stock (Invitrogen) solution, made in dimethyl sulfoxide] and 2 µL of PI (Invitrogen by Thermo Fisher Scientific, Carlsbad, CA, USA) solution 1 mg/mL were added simultaneously to 500 µL of sample, and incubated for 20 min in the dark. SYBR and SYTO9 are detected in the FITC-A channel and PI in the PC5.5-A channel.

All the light scatter and fluorescence signals were plotted in logarithmic-scale cytograms using CytExpert 2.4 software (Beckman Coulter, USA). The equipment was calibrated daily using a suspension of around 3 µm fluorospheres with an emission range from 410 to 800 nm (Beckman Coulter, CytoFLEX Daily QC Fluorospheres, Brea, CA, USA).

All samples, before FC analysis, were subjected to cellular ultrasonic disaggregation (TranssonicT660/H, Elma, Singen, Germany) for 10 s, at 35 kHz, followed by vigorous homogenization, to remove cell aggregates. The event flux was also adjusted to 300 events/s. For control, unstained cells were previously run in the FC to adjust the cells' autofluorescence to the first log decade in the fluorescence density plots (FITC versus PC5.5 channels). The autofluorescence adjustment in the density plots, focusing on the first logarithmic decade, improves the separation of stained and unstained cells by minimising the influence of background fluorescence. This approach involves setting the instrument's photomultiplier tube voltages so that unstained cells fall within the first log decade of the fluorescence scale, essentially "zeroing out" the autofluorescence background. This strategy allows for a clearer distinction between the fluorescence signals from stained cells and the inherent

autofluorescence of cells. FC controls were carried out using *C. vulgaris* cells under opposed physiological states as described by Taborda et al. [26]. For the control of cells with intact membranes (intact cells), an exponentially growing *C. vulgaris* culture was used as a positive control. A heat-treated *C. vulgaris* culture—prepared by incubating the cells in a boiling water bath at 100 °C for 30 min—was used as a negative control, as this treatment disrupts the cell membrane structure and results in fully permeabilized cells.

2.6. Protein and Carbohydrate Content

The protein content was assessed using the Kjeldahl method with a nitrogen-to-protein conversion factor of 6.25 [27]. The carbohydrate content was determined by quantitative acid hydrolysis of the biomass [28], followed by the phenol–sulfuric acid method [29] and spectrophotometry (490 nm) using the glucose standard curve.

2.7. Calculation of the Sedimentation Velocity of Chlorella vulgaris Cells

The velocity of sedimentation for an individual falling spherical particle in a diluted solution can be predicted using Stokes's equation [30], since *Chlorella* cells are spherical:

$$\mathbf{v_s} = \frac{\mathbf{2}}{\mathbf{9}} \times \frac{\Delta\rho}{\boldsymbol{\eta}} \times \mathbf{g} \times \mathbf{r_i}^{\mathbf{2}} \quad (1)$$

where v_s is the velocity of the spherical particle in water, Δρ is the density difference between the particle and the liquid, η is the viscosity of the liquid, g is the gravitational acceleration and r_i is the particle radius.

3. Results and Discussion

3.1. Previous Fluorescent Dye Selection

Figure 3 shows the histograms (cell count/FITC-A channel) concerning SYTOX, CFDA, SYBR/PI, and SYTO9/PI *C. vulgaris* cell staining. There were no significant changes between the SYTOX florescence emitted by untreated (intact cells) and heat-treated (permeabilised) *C. vulgaris* cells stained with SYTOX (Figure 3a), which means that SYTOX staining did not allow for differentiation between intact and permeabilised *C. vulgaris* cells. Indeed, variations in SYTOX staining, as well as difficulty in establishing intensity thresholds for separating live and dead cells in phytoplankton have been recorded for SYTOX [31].

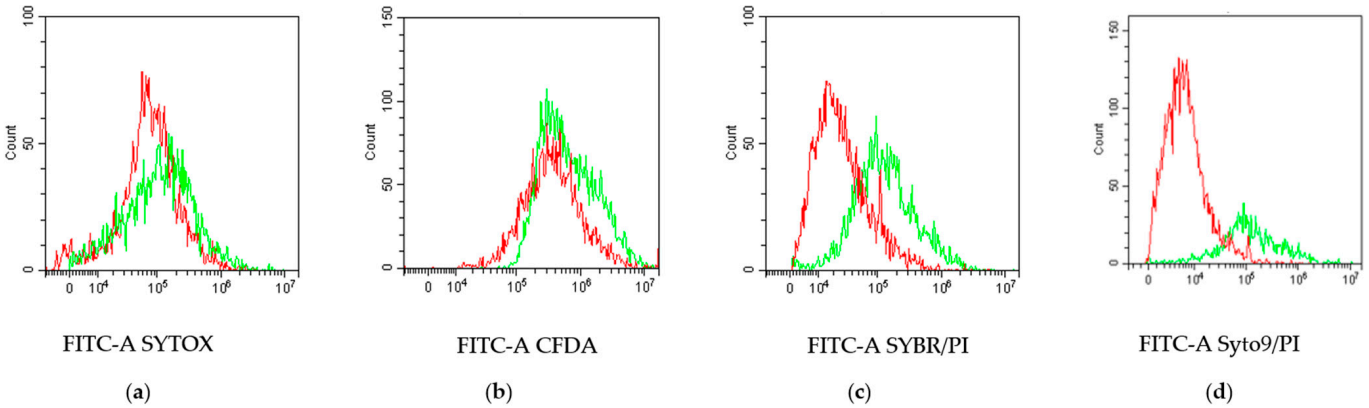

Figure 3. Untreated (green line) and heat-treated (red line) *C. vulgaris* cells developed on WWW stained with SYTOX (**a**); CFDA (**b**); SYBR + PI (**c**); SYTO9 + PI (**d**).

Reavie et al. [32] reported that SYTOX was unable to stain nuclei of *Scenedesmus* cells (small green algal species) in killed samples, and so dead cells were falsely identified as alive. In this work, the same was observed for *C. vulgaris* cells.

The fluorescence of untreated and treated CFDA-stained *C. vulgaris* cells is shown in Figure 3b. Despite the fluorescence of untreated cells being higher than that observed for treated cells (as expected, since the enzymatic system and membrane integrity of heat-treated cells were destroyed), the heat-treated cells were also stained with CFDA; therefore, the difference between treated and untreated cells' CFDA fluorescence peaks did not allow a good separation and thus a clear differentiation between intact cells with enzymatic activity from cells with no enzymatic activity. As far as we know, there are no published references on the use of CFDA for *Chlorella* cells. Nevertheless, this dye was successfully used to evaluate the enzymatic activity of *Tetradesmus obliquus* cells [33]. The difference between the behavior of *Chlorella vulgaris* and *Tetradesmus obliquus* cells, when stained with CFDA, was probably due to differences in the enzymatic activity system of each microalga; indeed, the latter showed higher esterase activity under those specific conditions, promoting CFDA conversion, resulting in an increase in cells' fluorescence.

The separation between treated and untreated cells was enhanced using SYBR/PI and SYTO9/PI double-staining (Figure 3c,d). However, the difference between the fluorescence peak maxima of treated and untreated cells was 850 for SYBR/PI, compared to 4900 for SYTO9/PI. This result demonstrates the higher efficiency of the latter procedure in distinguishing intact from permeabilized *C. vulgaris* cells. For this reason, the SYTO9/PI dual-staining method was selected for further monitoring of *C. vulgaris* cultivations.

3.2. FC Controls

A few cytometric controls were carried out before monitoring the microalgal cultivations on synthetic medium and WWW. The corresponding dot plots are shown in Figures 4–6, to demonstrate the efficacy of the staining protocol (SYTO9 + PI) in identifying *C. vulgaris* populations (shown as green dots) grown on non-sterile WWW (thus containing other microorganisms). The identification of *C. vulgaris* cells was based on the chlorophyll fluorescence signal emitted by the cells, detected in the APC-A channel. This population was shown in green, in the H2-UR quadrant, displayed in the APC-A/SSA density plots (Figure 4a). The orange population included other non-photosynthetic cells, debris and particles (noise) since they did not emit chlorophyll fluorescence.

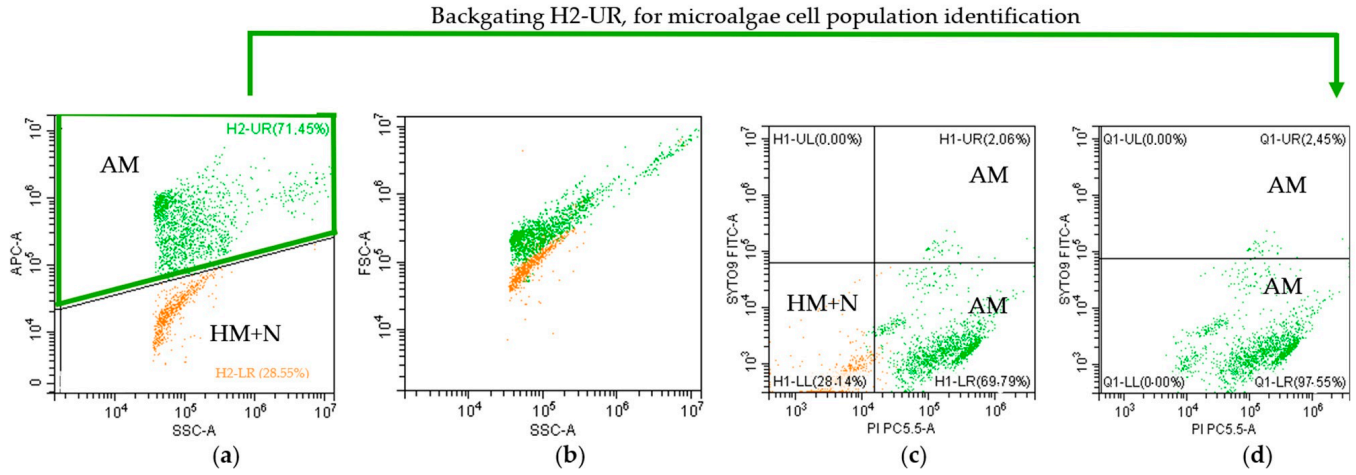

Figure 4. Flow cytometric controls for unstained and untreated exponentially growing *C. vulgaris* cells developed on WWW. (**a**) APC-A/SSC-A density plot; (**b**) FSC-A/SSC-A density plot; (**c**) FITC-A/PC5.5-A (SYTO9/PI) density plot; (**d**) FITC-A/PC5.5 (SYTO9/PI) density plot, after H2-UR quadrant (from Figure 4a) backgating. AM—autotrophic microalgae; HM—heterotrophic microorganisms; N—noise; green population: autotrophic microalgae cells; orange population: heterotrophic cells and noise.

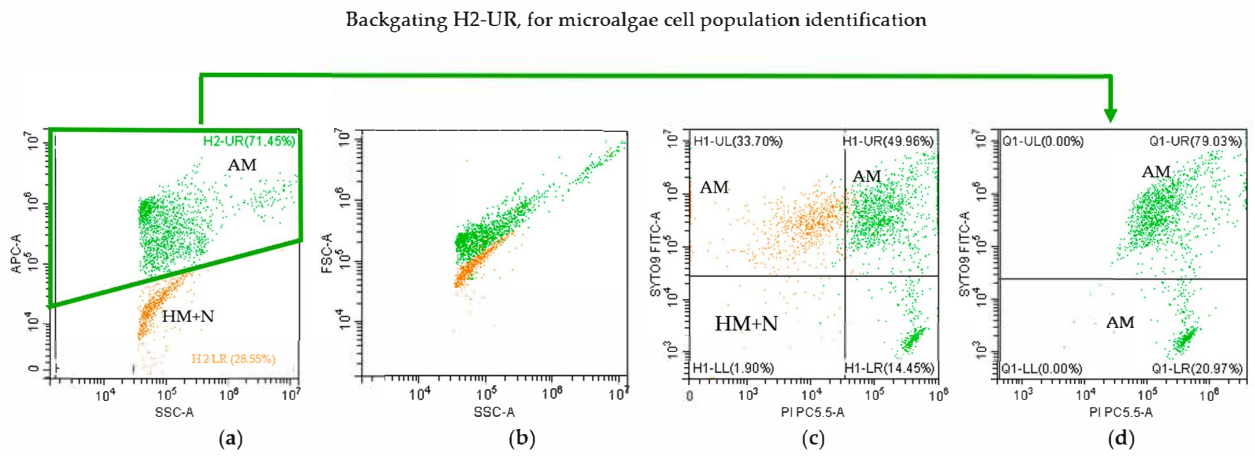

Figure 5. Flow cytometric controls for SYTO9+PI-stained and untreated exponentially growing *C. vulgaris* cells developed on WWW. SYTO9/PI density plots: (**a**) APC-A/SSC-A density plot; (**b**) FSC-A/SSC-A density plot; (**c**) FITC-A/PC5.5 (SYTO9/PI) density plot; (**d**) FITC-A/PC5.5 (SYTO9/PI) density plot, after H2-UR quadrant (shown in Figure 5a) backgating. AM—autotrophic microalgae; HM—heterotrophic microorganisms; N—noise; green population: autotrophic microalgae cells; orange population: heterotrophic cells and noise.

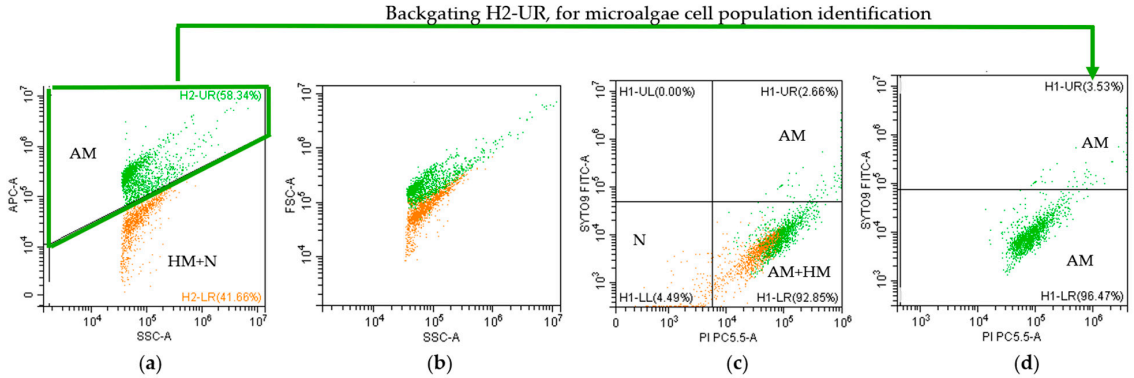

Figure 6. Flow cytometric controls for SYTO9/PI-stained and heat-treated exponentially growing *C. vulgaris* cells developed on WWW. (**a**) APC-A/SSC-A density plot; (**b**) FSC-A/SSC-A density plot; (**c**) FITC-A/PC5.5 (SYTO9/PI) density plot; (**d**) FITC-A/PC5.5 (SYTO9/PI) density plot, after H2-UR quadrant (from Figure 6a) backgating. AM—autotrophic microalgae; HM—heterotrophic microorganisms; green population: autotrophic microalgae cells; orange population: heterotrophic cells and noise.

Backgating is a valuable technique in FC used for identifying specific cell populations. It enables the confirmation of staining patterns or gating strategies by tracking the selected population across different parameter plots using specialised software. In this study, backgating was applied to highlight and identify the microalgal population in various density plots using the CytExpert 2.4 software. By applying the H2-UR quadrant defined in Figure 4a, the *C. vulgaris* population (shown in green) was successfully visualised in the FSC-A (cell size) versus SSC-A (internal complexity) plots (Figure 4b). This demonstrated the clear differentiation between the autotrophic microalgae cell population and other microbial populations and noise. The orange population should include mostly bacteria and yeast, since they show an FSC (size) profile lower than the microalgae cells (green spot), as depicted in Figure 4b. In this plot (FSC-A/SSC-A), the microalgal cells appeared as a comet shape, typical of a population containing events with different sizes and internal complexities. Indeed, *C. vulgaris* cells show different sizes and shapes when grown in a liquid medium, since the cells are in different growth stages (mother and daughter cells, the

latter being smaller with lower FSC/SSC signals, and the former being bigger, displaying higher FSC/SSC signals) [34]. In these plots, the orange population also appeared as a comet, indicating that those cells also had different sizes and internal complexities, which supports that this population is composed of different types of microorganisms and particles.

A sample from the exponential culture was run without stains, displaying autofluorescence, as shown in Figure 4a–d. Most of the untreated autotrophic microalgae cells (69.79%, Figure 4c) depicted a higher signal in the PC5.5 detector, as a result of their chlorophyll content (which was also detected in this channel), and a low signal detected in the FITC-A channel, located in the lower right quadrant H1-LR (Figure 4c), indicating that they did not produce pigments that emitted fluorescence at those wavelengths (525/40 nm). The non-photosynthetic microorganisms and noise appeared in the lower left quadrant (H1-LL) since they do not produce chlorophyll (Figure 4c). Applying quadrant H2-UR (from Figure 4a) to the dot plot FITC/PC5.5 (Figure 4c), only the target microalgal population appeared (Figure 4d).

When the exponentially growing culture was stained with SYTO9/PI, the density plots APC-A/SSC-A (Figure 5a) and FSC-A/SSC-A (Figure 5b) were the same as those obtained for unstained cells (Figure 4a,b) since these cells were not exposed to any treatment. Most of the microalgae cells were double-stained with SYTO9 and PI (49.96%, H1-UR quadrant, Figure 5c), indicating that these cells had intact membranes. Most of the non-photosynthetic cell population (33.70%, H1-UL) was also double-stained with SYTO9 and PI, which showed that they had intact membranes. Noise (1.90%) was also revealed in Figure 5c, corresponding to material that was not stained by any of those stains (cell debris and medium particles). Figure 5d resulted from the application of quadrant H2-UR (Figure 5a) to Figure 5c, just showing the microalgal population: 79.03% of the cells had intact membranes and 20.97% had permeabilised membranes. This result was expected, since exponentially growing cultures may contain cells from the fully metabolically active state to death, resulting from a few factors, such as fast growth, medium pH changes, inhibitor metabolites, etc. [35].

Comparing the chlorophyll fluorescence emitted by untreated (Figure 4a) and heat-treated C. vulgaris cells (Figure 6a), a decrease of 97% in the APC-A fluorescence signal was recorded when the cells were heat-treated (untreated cells' APC-A fluorescence signal: 666,514.6, quadrant H2-UR, Figure 4a); (heat-treated cells' APC-A fluorescence signal: 22,415.1, quadrant H2-UR in Figure 6a), which means, as expected, that the heat treatment denatured the chlorophyll pigment. The dot plot of the heat-treated sample stained with SYTO9/PI (Figure 6c) showed a major population (92.95%) located in the H1-LR quadrant, which was stained with PI, but not with SYTO9, corresponding to all the microbial cells with permeabilised membranes. The percentage of events identified as noise (4.49%) located in the H1-LL quadrant increased compared to the untreated sample (1.90%, Figure 5a), due to the cell debris resulting from cell lysis. By backgating, applying the H2-UR quadrant (Figure 6a) to the FITC/PC5.5 plot (Figure 6c), only the microalgal population is shown, with almost all the permeabilised cells located in the H1-LR quadrant (96.47%, Figure 6d) due to the harsh heat treatment which collapsed the cell membrane.

These controls allowed the identification of all the events, based on the chlorophyll fluorescence detected in the APC-A channel, which allowed us to differentiate the microalgal population from other events such as non-photosynthetic microorganisms, medium particles and debris; in addition, FC coupled with the SYTO9 and PI double-staining protocol also allowed us to distinguish intact from permeabilised cells. These protocols were further used to monitor the cultures developed on WWW, in the 100L bubble column and the 750 L raceway.

3.3. Outdoor Raceway Experiments

The two raceway ponds of 750 L (working volume of 270 L), containing synthetic medium (control) and WWW, were inoculated with *C. vulgaris* and monitored over 33 days (Figure 7). The cell number profiles were similar, reaching approximately 1.54×10^6 cells/mL for the control and 1.64×10^6 cells/mL for the WWW cultivation (Figure 7a), indicating that both media, when supplemented with $NaNO_3$ and K_2HPO_4, supported comparable final biomass concentrations.

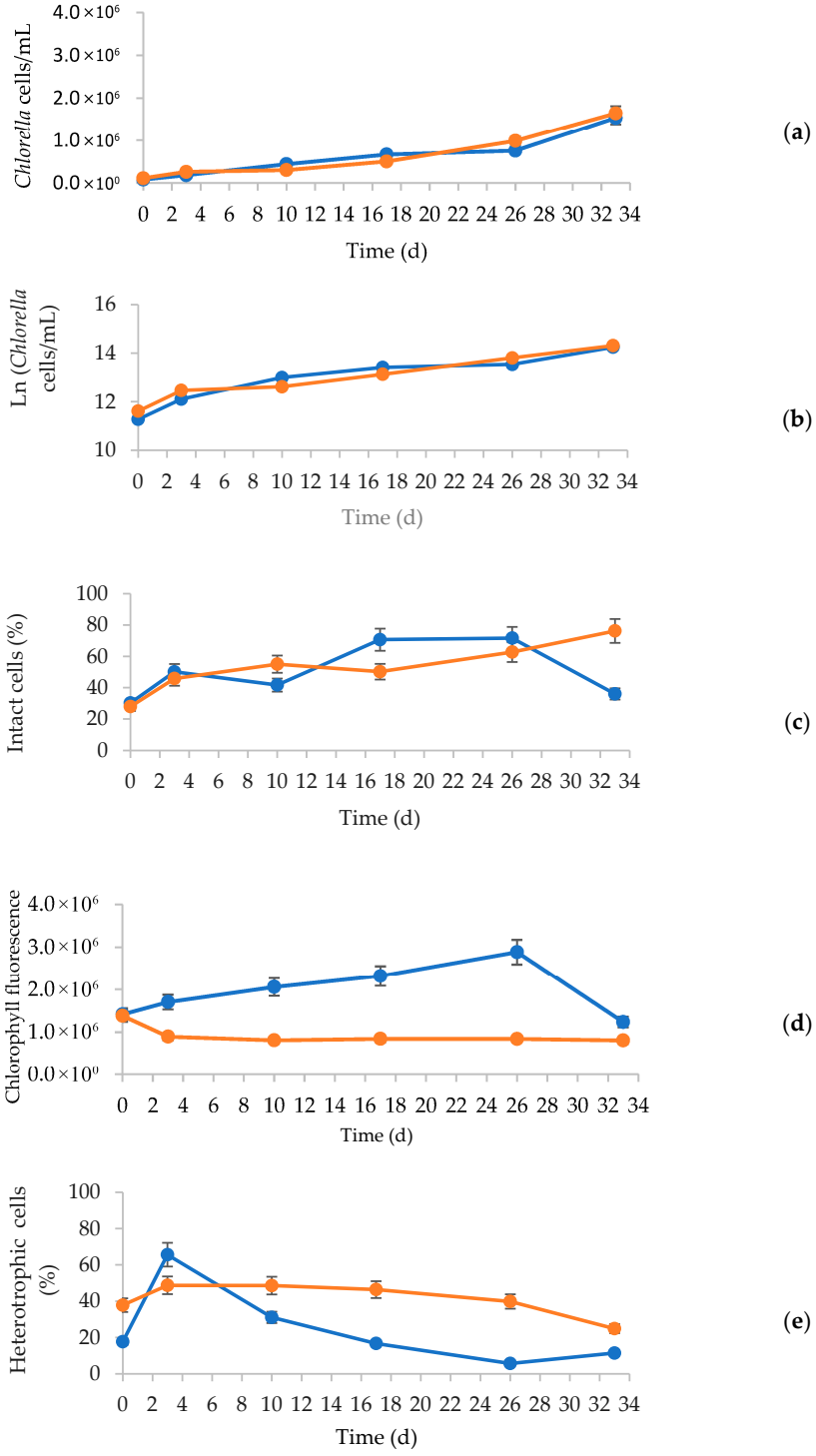

Figure 7. Raceway cultivation profiles: *C. vulgaris* cell count (**a**); natural logarithmic of *C. vulgaris* cell count (**b**); percentage of intact cells (**c**); chlorophyll fluorescence (**d**); percentage of heterotrophic cells (**e**). Blue line: control (synthetic medium); orange line: WWW medium.

The initial period (up to t = 3 d) was marked by faster cell growth in both cultures, suggesting favourable starting growth conditions. However, after this stage, both cultures grew slower (Figure 7b), which suggests possible limitations in nutrients such as CO_2, light or others. This pattern is commonly observed in microalgal cultures under nutrient-limited conditions [36]. For the control assay, the percentage of intact cells increased up to 71.63% (t = 26 d), having decreased to 36.03% (Figure 7c). This percentage increased over the WWW cultivation, attaining 76.2% at the end of the assay.

In the control cultivation, the chlorophyll fluorescence peaked at 2.89×10^6 at t = 26 d, then sharply declined to 1.24×10^6 by the end of the assay. This indicates a reduction in the microalgae autotrophic metabolic activity at that time, likely due to inorganic carbon limitation, as no air or CO_2 supplementation was provided during the raceway experiments. This limitation may have triggered partial cell lysis by the end of the assay, as supported by the ≈64% proportion of damaged cells observed at t = 33 d (Figure 7c). Cell lysis could have released organic carbon into the medium, enabling a metabolic shift of *C. vulgaris* from autotrophy to heterotrophy. Indeed, *C. vulgaris* is known for its nutritional flexibility, being capable of switching to mixotrophic or heterotrophic metabolism under suitable conditions [37]. The increase in cell number observed at t = 33 d for the control raceway (Figure 7a) may thus be attributed to heterotrophic growth supported by organic carbon released from lysed cells. Overall, the chlorophyll fluorescence values were much higher for the control than for the WWW cultivation, demonstrating that the synthetic medium promoted the autotrophic metabolism, unlike WWW cultivation, which showed more stable and lower chlorophyll fluorescence values throughout the entire assay (8.44×10^5 at t = 33 d, Figure 7d). This result was expected, since the control medium did not contain organic carbon, while WWW contained a high organic carbon load, as previously mentioned, promoting a shift toward heterotrophic metabolism. Additionally, the presence of suspended particles and other microorganisms in the non-sterile WWW cultivation likely reduced light penetration, because these suspended solids and microorganisms can absorb and scatter light, creating shading effects and limiting the amount of light reaching the microalgae cells, further limiting the photosynthetic activity of *C. vulgaris* [38].

As expected, throughout most of the cultivation period, the percentage of heterotrophic cells was higher in the WWW cultures than in the control (Figure 7e), likely due to the presence of organic carbon and reduced light penetration caused by suspended solids in the WWW. These conditions favoured the proliferation of heterotrophic microorganisms and promoted a shift in *C. vulgaris* metabolism toward heterotrophy or mixotrophy, reducing reliance on photosynthesis—an effect supported by the consistently low chlorophyll fluorescence signals observed throughout the WWW cultivation (Figure 7d).

3.4. Outdoor Bubble Column Experiment

The bubble column cultures reached 2.85×10^5 cells/mL and 2.30×10^6 cells/mL for the control and WWW cultivations, respectively, at the end of the assay (t = 33 d, Figure 8a). Both values were higher than those obtained for the raceway cultivations (1.54×10^6 and 1.64×10^6 cells/mL for the control and WWW assays, respectively, at the end of the assays; Figure 7a). Both cultures entered the stationary phase at t = 17 d, achieving a plateau, typical of a limitation due to total nutrient starvation (most probably nitrogen) (Figure 8b).

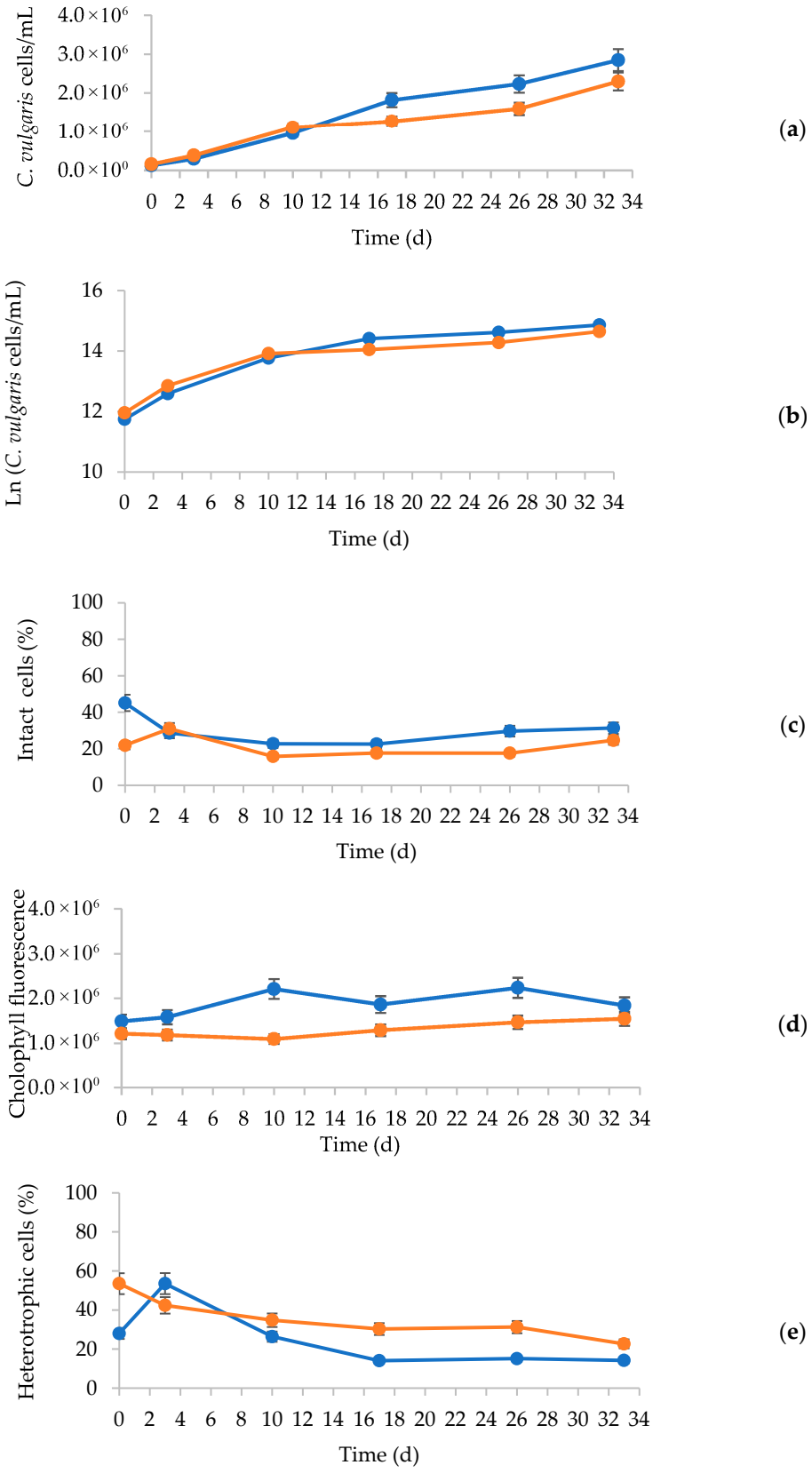

Figure 8. Bubble column cultivation profiles: cell count (**a**); natural logarithm of cell count (**b**); percentage of intact cells (**c**); chlorophyll fluorescence (**d**); percentage of heterotrophic cells (**e**). Blue line: control (synthetic medium); orange line: WWW medium.

The proportion of intact cells was always below 50% during the entire time course of both assays (Figure 8c), indicating that the cells were exposed to more adverse con-

ditions during the evolution of both cultivations, compared to the raceway cultivations (Figure 7c). Several factors might have contributed to the microalgae cells' stress response. Firstly, the nutrient starvation referred to above might have been responsible for the lower proportion of intact cells, a condition that did not occur in the raceway cultivations, as already mentioned, since the cells did not enter the stationary phase (Figure 7b). Secondly, shear stress might have contributed to the lower proportion of intact *Chlorella* cells, as reported by Khoo et al. [39], Wang and Lan [40] and Zhang et al. [41]. Shear stress is a type of hydrodynamic stress generated by mixing and/or aeration, critical when considering microalgal cultivations, since microalgal cell walls and membranes may be affected by this condition. Shear stress is generated when aerating and mixing a liquid medium, both essential for successful microalgal cultures, and particularly important for large-scale microalgal farming. However, excessive shear stress can cause severe cell damage which can culminate in cell lysis, reducing the biomass productivity [40]. For this reason, cells grown in bubble columns, in which the gas phase is dispersed into the liquid medium in the form of bubbles by means of a gas sparger placed in the bottom of the column, are usually exposed to higher shear stress levels than in raceways due to bubbles rising and bursting [40,42,43]. These two factors explain the lower intact cell percentage recorded for both bubble columns, compared to the raceway cultivations (Figures 7c and 8c).

As expected, the chlorophyll fluorescence values were always higher for the control than for the WWW bubble column (1.83×10^6 and 1.54×10^6, at the end of the control and WWW cultivations, respectively; Figure 8d) since the control medium did not contain organic carbon, nor particles, and was clearer than WWW, thus allowing more efficient light penetration, conditions that promoted the autotrophic metabolism.

The higher proportion of heterotrophic cells present in the WWW bubble column compared to the control—22.70% versus 14.2% at the end of the cultivation—(Figure 8e) supports the conclusion that the synthetic medium favoured the autotrophic metabolism as it lacked organic carbon.

3.5. Comparison Between Control and WWW Cultivations Across Raceway and Bubble Column Systems

The cultivation of *C. vulgaris* under different reactor configurations and media revealed distinct physiological and metabolic behaviours.

Bubble column systems supported higher *C. vulgaris* cell concentrations than raceways (Figures 7a and 8a), likely due to more efficient mass transfer and improved CO_2 availability, as previously reported by Assunção and Malcata [43] and Zhang et al. [41]. In addition, bubble columns promote more effective light penetration compared to raceway systems, owing to their greater illuminated surface area. The vertical, cylindrical geometry of bubble columns allows light to enter from both the lateral and top surfaces of the liquid column, whereas raceways are primarily illuminated from the top surface only [40].

The proportion of intact cells was consistently lower in the bubble column cultures (generally <31%) compared to the raceway cultivations (Figures 7c and 8c), regardless of the medium used. This difference can be attributed primarily to the higher shear stress conditions in the bubble column system, as mentioned above. In contrast, the raceways, mechanically mixed using paddle wheels, generated lower shear forces, thus providing a gentler environment for microalgae. As a result, the raceway cultures maintained higher proportions of cells with intact membranes (mostly >45%) throughout the cultivation period.

Regarding the media used, control assays, grown on synthetic medium (without organic carbon) mostly promoted autotrophic metabolism, as evidenced by higher chlorophyll fluorescence values detected by FC, in both systems (Figures 7d and 8d). In contrast, WWW cultures—rich in organic compounds such as sugars, acetate, and lactic acid—showed lower chlorophyll fluorescence signals, suggesting a shift toward mixotrophic or heterotrophic

metabolism, where reliance on photosynthesis is reduced [21,37]. This is consistent with the high proportion of heterotrophic cells found in both WWW assays. Indeed, the visual colour differences observed between the two cultivations (Figures 1 and 2)—a greener appearance in the control cultures and a browner tone in the WWW cultures—were consistent with the chlorophyll fluorescence data obtained by FC. The higher chlorophyll fluorescence in both control assays explains their more intense green coloration, whereas the lower chlorophyll content and the presence of naturally coloured compounds in the WWW medium (e.g., polyphenols, tannins, and fermentation by-products) likely contributed to the browner appearance of those cultures.

Although all assays were inoculated with the same *C. vulgaris* culture, the distinct media compositions likely promote different growth conditions that drove different microbial dynamics at the beginning of the assays (t = 3d, Figures 7e and 8e). The control medium, being synthetic and free of inhibitory compounds, possibly offered a favourable environment for opportunistic heterotrophic microorganisms to rapidly proliferate during the early phase of cultivation. This heterotrophic bloom, shown as a sharp peak at t = 3 d (Figures 7e and 8e), could have been supported by organic carbon released from the algal inoculum, in the form of cell debris or exudates. As *C. vulgaris* grew and altered the environment (e.g., by changing pH, depleting nutrients, or producing metabolites), the availability of the organic carbon decreased, leading to the observed decline in heterotrophic cell proportions after t = 3 d in the control cultivations. In contrast, WWW, although rich in organic carbon (e.g., sugars and acids), also contains inhibitory compounds—such as polyphenols, ethanol, and acidic components—known to suppress or delay heterotrophic microbial growth. These conditions might have prevented the early peak of heterotrophs but allowed a more sustained and stable heterotrophic population throughout the cultivation, as observed in Figures 7e and 8e.

Altogether, these comparisons highlight the importance of both reactor configuration and medium composition in shaping microalgal physiology and overall process performance. While WWW supplies nutrients that support microalgal growth, reactor-specific constraints must be considered to optimise productivity and harvesting efficiency.

3.6. Changes in the Microalgae Cell Size

Samples collected from the bubble column and raceway cultivations were analysed in terms of cell size (FSC) and internal complexity (SSC) at the beginning (t = 0 d) and end (t = 33 d) of all the assays (Figure 5).

All FSC and SSC signal profiles were similar and below 45 at the beginning of the cultivations (Supplementary Material Figure S1a,b).

At t = 33 d, both control experiments showed broader FSC and SSC profiles than the WWW cultivations (Supplementary Material Figure S1c,d), indicating that, at that time, cells with different sizes and internal complexities were present. Indeed, the life cycle of *Chlorella vulgaris* comprises the following stages: (i) early cell growth phase; (ii) late cell growth phase; (iii) early cell division phase; (iv) late cell division phase; (v) daughter cell maturation phase; and (vi) autospore release phase [44]. During all these stages, the microalgae cells changed their size and internal complexity. Indeed, dividing cells (in the division phases (iii) and (iv)) show higher size and internal complexity, and thus higher FSC and SSC signals, respectively, due to their higher DNA content, compared to daughter cells and autospores (phases (i)–(vi)) [35]. On the contrary, sharper FSC and SSC peaks were detected for the WWW cultivations (Supplementary Material Figure S1c,d), revealing that, in this case, the microalgae cells had similar sizes and complexities, indicating lower microalgae cell growth stage diversification. Since lower FSC and SSC signals were detected for the cells grown on control cultures at t= 33 d, they might have been present in these

cultures in the early stages of the cell cycle (stages (i) and (ii)) with lower size (FSC) and internal complexity (SSC). This suggests that the control assays might have contained fewer microalgae cells in stages (iv)–(vi) than the WWW assays at the end of the experiments (t = 33 d).

In addition, significant differences between the FSC signals of cells collected from the raceway and the bubble column grown on WWW cultures were detected at t = 33 d. Until t = 10 d, *C. vulgaris* cells' FSC signals (proportional to cell size) were similar in both systems, but from that day onwards, these signals were higher for the cells grown on the bubble column than in the raceway cultivation (Supplementary Material Figure S2). At t = 33 d, the mean FSC signal for the cells grown in the bubble column was 374,944.1 au, and for the raceway, it was 455,946.0 au (Supplementary Material Figure S2), which indicated that cells grown in the former system became larger in size (and thus, in diameter, since *Chlorella* cells are spherical) than those grown in the bubble column, corresponding to a difference of 22%. This difference might be due to the different growth phases of *Chlorella* cells cultivated in the raceways and bubble columns. As mentioned above, at the end of the cultivations (t = 33 d), the microalgae cell counts for both raceway cultivations were still increasing (Figure 7b) while the cell counts observed for both bubble columns cultivations reached a plateau (at t = 17 d, Figure 8b). According to Chioccioli et al. [45], when *Chlorella* cells reached the stationary phase, they increased their diameter, and thus their size. Therefore, the different *Chlorella* growth phases observed in the raceways and bubble columns at the end of the experiments explained the different cell sizes observed for the two cultivation systems. According to the above results, the radius of *Chlorella* cells grown in the bubble column is 22% larger than the radius of *Chlorella* cells grown in the raceway.

Therefore, according to Equation (1),

$$r_{bubble\ column} \propto 1.22 \times r_{raceway} \tag{2}$$

$$\frac{(v_s)_{bubble\ column}}{(v_s)_{\ raceway}} \propto \frac{(1.2 \times r_{raceway})^2}{(r_{raceway})^2} \tag{3}$$

$$\frac{(v_s)_{bubble\ column}}{(v_s)_{\ raceway}} \propto 1.49 \tag{4}$$

in which $r_{bubble\ coum}$ is the radius of *Chlorella* cells grown in the bubble column, $r_{raceway}$ is the radius of *Chlorella* cells grown in the raceway, $(v_s)_{bubble\ column}$ is the velocity of the *Chlorella* cells grown in the bubble column, and $(v_s)_{raceway}$ is the velocity of the *Chlorella* cells grown in the raceway.

Based on the above equations, it was concluded that the sedimentation velocity of the *Chlorella* cells grown in the bubble column was 49% higher than that of the *Chlorella* cells grown in the raceway cultivation, which is a significant increase in terms of sedimentation velocity. Thus, these results demonstrate that the microalgae cell size indeed has a direct impact on the sedimentation velocity.

Microalgae cell size plays a crucial role in downstream processing and microalgal biotechnology, as it directly influences the microalgal biomass harvesting efficiency. Larger cells sediment more readily, making them easier to separate from the culture medium than smaller cells, thereby reducing processing costs [46,47].

The SSC profiles of the cells collected from both systems were coincident without changes throughout the cultivations, indicating that no changes occurred at the cell internal complexity level.

In the present study, the two systems—raceways and bubble columns—produced *C. vulgaris* cells of different sizes when grown on WWW, which can significantly impact

the overall process costs associated with each cultivation. Thus, monitoring cell size throughout microalgal cultivations is essential for optimising downstream operations and overall process efficiency.

3.7. Biomass Characterisation

The biomass collected at the end of the bubble column cultivations contained a higher carbohydrate content (>49%) compared to the raceway cultivations (<32%) (Figure 9). Conversely, the protein content was higher in the raceway biomass (>48%) than in the bubble column biomass (<44%). This pattern is consistent with the probable nitrogen limitation in the bubble column cultures, as proteins contain nitrogen along with carbon, hydrogen, and oxygen. The lower nitrogen availability may explain the elevated carbohydrate accumulation in the bubble column biomass.

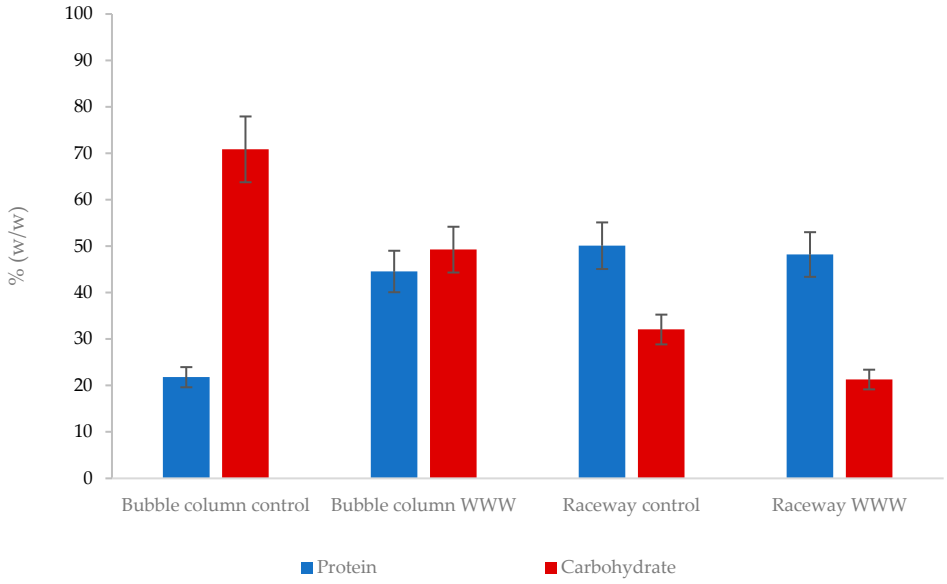

Figure 9. Composition of the biomass collected at the end of the raceway and bubble column cultivations.

Despite these differences, biomass from both cultivation systems grown on WWW contained over 40% protein (*w*/*w*), making it suitable for potential applications such as animal feed, biofertilizers, and biogas production [48]. The carbohydrate and protein contents observed here are higher than those reported by [49] for a mixed culture of *Arthrospira platensis* and *C. vulgaris* grown on 20% diluted WWW in an open pond, which showed 12% and 8% carbohydrate and protein, respectively. Zkeri et al. [1] reported a 59% protein content in *C. sorokiniana* biomass from sequential-batch cultures on WWW in shake flasks, possibly reflecting differences in the wastewater composition.

As mentioned above, no sterilisation was applied to the culture media or systems to simulate realistic large-scale outdoor conditions with complex substrates such as WWW. Consequently, microbial consortia were present throughout cultivation. While non-axenic conditions introduce biological variability, they mirror the reality of industrial-scale microalgae production. In addition, co-cultivating microalgae with heterotrophic microorganisms can foster synergistic interactions [50]. However, these benefits must be balanced against risks such as competition for nutrients, accumulation of unwanted metabolites, or contamination by pathogens, which could compromise biomass quality—especially for feed or food uses.

4. Conclusions

FC was successfully applied to monitor *C. vulgaris* cultivated on WWW in two outdoor systems—a 750 L raceway and a 100 L bubble column. This technique enabled the near-real-time assessment of cell concentration, membrane integrity, chlorophyll content and cell size, providing early indicators of cellular stress. It thus stands out as a powerful decision-support tool for dynamic microalgae cultivation on complex effluents.

WWW proved to be a promising culture medium, supplying water, organic carbon, and naturally occurring nutrients that reduced the need for synthetic inputs. Although some supplementation was necessary, WWW improved microalgal cultivation's sustainability and supported circular economy principles. Biomass produced in WWW cultivations contained over 40% protein, underscoring its potential for animal feed or other bioproduct applications.

Future work should explore FC's integration with large-scale photobioreactors and investigate the impact of microbial consortia on biomass quality, safety, and valorisation in food, feed, and bio-based sectors.

Supplementary Materials: The following supporting information can be downloaded at: https://www.mdpi.com/article/10.3390/fermentation11080442/s1, Figure S1: FSC and SSC histograms for *C. vulgaris* cells collected from all the assays at t = 0 d and t = 33 d. (a) and (b): FSC and SSC signals at t = 0 d; (c) and (d): FSC and SSC signals at t = 33 d. Navy blue line: Raceway control; Turquois line: Raceway WWW; Burgundy line: Bubble column control; Pink line: Bubble column WWW; Figure S2: FSC histograms for *C. vulgaris* cells collected from cultivations using WWW in the bubble column (green line) and in the raceway (red line). Samples collected at t = 0 d (a), 3 d (b), 10 d (c), 17d (d), 26 d (e), 33 d (f). Green line: Bubble column cultivation on WWW; Red line: Raceway cultivation on WWW.

Author Contributions: Conceptualisation, A.R. and T.L.d.S.; methodology, T.A.S., B.R., B.T.F., T.L.d.S. and A.R.; validation, T.A.S., B.R., B.T.F., T.L.d.S. and A.R.; resources, A.R.; writing—original draft preparation, T.L.d.S.; writing—review and editing, T.A.S., B.R., B.T.F., T.L.d.S. and A.R.; supervision, A.R. and T.L.d.S.; project administration, A.R.; funding acquisition, A.R. All authors have read and agreed to the published version of the manuscript.

Funding: This research was carried out under the REDWINE project "Increasing microalgae biomass feedstock by valorising wine gaseous and liquid residues", which has received funding from Bio-based Industries Joint Undertaking under the European Union's Horizon 2020 research and innovation programme under grant agreement No. 101023567.

Data Availability Statement: The original contributions presented in this study are included in the article. Further inquiries can be directed to the corresponding author(s).

Acknowledgments: The authors thank Graça Gomes and Natércia Santos for their valuable support in the analytical techniques.

Conflicts of Interest: The authors declare no conflicts of interest.

Abbreviations

WWW	Winery wastewater
FC	Flow cytometry
SYTOX	SYTOX Green
CFDA	Carboxyfluorescein diacetate
SYBR	SYBR GREEN I
PI	Propidium iodide
FSC	Forward scatter
SSC	Side scatter
FSC-A	Forward scatter area (detector)
SSC-A	Side scatter area (detector)

References

1. Zkeri, E.; Mastori, M.; Xenaki, A.; Kritikou, E.; Kostakis, M.; Dasenaki, M.; Maragou, N.; Fountoulakis, M.S.; Thomaidis, N.S.; Stasinakis, A.S. Winery Wastewater Treatment by Microalgae Chlorella Sorokiniana and Characterization of the Produced Biomass for Value-Added Products. *Environ. Sci. Pollut. Res.* **2024**, *31*, 49244–49254. [CrossRef]
2. Moreira, F.C.; Boaventura, R.A.R.; Brillas, E.; Vilar, V.J.P. Remediation of a Winery Wastewater Combining Aerobic Biological Oxidation and Electrochemical Advanced Oxidation Processes. *Water Res.* **2015**, *75*, 95–108. [CrossRef]
3. Marchão, L.; Fernandes, J.R.; Sampaio, A.; Peres, J.A.; Tavares, P.B.; Lucas, M.S. Microalgae and Immobilized TiO2/UV-A LEDs as a Sustainable Alternative for Winery Wastewater Treatment. *Water Res.* **2021**, *203*. [CrossRef]
4. Miklas, V.; Touš, M.; Miklasová, M.; Máša, V.; Horňák, D. Winery Wastewater Treatment Technologies: Current Trends and Future Perspective. *Chem. Eng. Trans.* **2022**, *94*, 847–852. [CrossRef]
5. Spennati, E.; Mirizadeh, S.; Casazza, A.A.; Solisio, C.; Converti, A. Chlorella Vulgaris and Arthrospira Platensis Growth in a Continuous Membrane Photobioreactor Using Industrial Winery Wastewater. *Algal Res.* **2021**, *60*, 102519. [CrossRef]
6. Latessa, S.H.; Hanley, L.; Tao, W. Characteristics and Practical Treatment Technologies of Winery Wastewater: A Review for Wastewater Management at Small Wineries. *J. Environ. Manag.* **2023**, *342*, 118343. [CrossRef]
7. Bolzonella, D.; Papa, M.; Da Ros, C.; Anga Muthukumar, L.; Rosso, D. Winery Wastewater Treatment: A Critical Overview of Advanced Biological Processes. *Crit. Rev. Biotechnol.* **2019**, *39*, 489–507. [CrossRef]
8. Spennati, E.; Casazza, A.A.; Converti, A. Winery Wastewater Treatment by Microalgae to Produce Low-Cost Biomass for Energy Production Purposes. *Energies* **2020**, *13*, 2490. [CrossRef]
9. Asadi, P.; Rad, H.A.; Qaderi, F. Comparison of Chlorella Vulgaris and Chlorella Sorokiniana Pa.91 in Post Treatment of Dairy Wastewater Treatment Plant Effluents. *Environ. Sci. Pollut. Res.* **2019**, *26*, 29473–29489. [CrossRef]
10. Miazek, K.; Remacle, C.; Richel, A.; Goffin, D. Effect of Lignocellulose Related Compounds on Microalgae Growth and Product Biosynthesis: A Review. *Energies* **2014**, *7*, 4446–4481. [CrossRef]
11. Ali, S.S.; El-Sheekh, M.; Manni, A.; Ruiz, H.A.; Elsamahy, T.; Sun, J.; Schagerl, M. Microalgae-Mediated Wastewater Treatment for Biofuels Production: A Comprehensive Review. *Microbiol. Res.* **2022**, *265*. [CrossRef]
12. Sarma, U.; Hoque, M.E.; Thekkangil, A.; Venkatarayappa, N.; Rajagopal, S. Microalgae in Removing Heavy Metals from Wastewater—An Advanced Green Technology for Urban Wastewater Treatment. *J. Hazard. Mater. Adv.* **2024**, *15*, 100444. [CrossRef]
13. Blanchard, M.; Teil, M.J.; Ollivon, D.; Legenti, L.; Chevreuil, M. Polycyclic Aromatic Hydrocarbons and Polychlorobiphenyls in Wastewaters and Sewage Sludges from the Paris Area (France). *Environ. Res.* **2004**, *95*, 184–197. [CrossRef]
14. Xiong, J.Q.; Kurade, M.B.; Jeon, B.H. Can Microalgae Remove Pharmaceutical Contaminants from Water? *Trends Biotechnol.* **2018**, *36*, 30–44. [CrossRef]
15. Morais, E.G.; Cristofoli, N.L.; Maia, I.B.; Magina, T.; Cerqueira, P.R.; Teixeira, M.R.; Varela, J.; Barreira, L.; Gouveia, L. Microalgal Systems for Wastewater Treatment: Technological Trends and Challenges towards Waste Recovery. *Energies* **2021**, *14*, 8112. [CrossRef]
16. Hewitt, C.J.; Nebe-Von-Caron, G. The Application of Multi-Parameter Flow Cytometry to Monitor Individual Microbial Cell Physiological State. *Adv. Biochem. Eng. Biotechnol.* **2004**, *89*, 197–223. [CrossRef]
17. Hyka, P.; Lickova, S.; Přibyl, P.; Melzoch, K.; Kovar, K. Flow Cytometry for the Development of Biotechnological Processes with Microalgae. *Biotechnol. Adv.* **2013**, *31*, 2–16. [CrossRef]
18. Foladori, P.; Petrini, S.; Bruni, L.; Andreottola, G. Bacteria and Photosynthetic Cells in a Photobioreactor Treating Real Municipal Wastewater: Analysis and Quantification Using Flow Cytometry. *Algal Res.* **2020**, *50*, 101969. [CrossRef]
19. Park, K.H.; Jho, E.H.; Hwang, S.J. Quantitative Viability Assessment of Microalgae for Advanced Wastewater Treatment by Flow Cytometry. *KSCE J. Civ. Eng.* **2023**, *27*, 3714–3719. [CrossRef]
20. Freitas, C.; Parreira, T.M.; Roseiro, J.; Reis, A.; Da Silva, T.L. Selecting Low-Cost Carbon Sources for Carotenoid and Lipid Production by the Pink Yeast Rhodosporidium Toruloides NCYC 921 Using Flow Cytometry. *Bioresour. Technol.* **2014**, *158*, 355–359. [CrossRef]
21. Li, X.; Shen, X.; Jiang, W.; Xi, Y.; Li, S. Comprehensive Review of Emerging Contaminants: Detection Technologies, Environmental Impact, and Management Strategies. *Ecotoxicol. Environ. Saf.* **2024**, *278*, 116420. [CrossRef]
22. Čertnerová, D.; Galbraith, D.W. Best Practices in the Flow Cytometry of Microalgae. *Cytom. Part A* **2021**, *99*, 359–364. [CrossRef]
23. Haberkorn, I.; Off, C.L.; Besmer, M.D.; Buchmann, L.; Mathys, A. Automated Online Flow Cytometry Advances Microalgal Ecosystem Management as in Situ, High-Temporal Resolution Monitoring Tool. *Front. Bioeng. Biotechnol.* **2021**, *9*, 1–13. [CrossRef]
24. Barteneva, N.S.; Kussanova, A.; Dashkova, V.; Meirkhanova, A.; Vorobjev, I.A. *Spectral and Imaging Cytometry*; Springer: Berlin/Heidelberg, Germany, 2023; Volume 2635, Chapter 2; pp. 23–40. [CrossRef]
25. Ihadjadene, Y.; Walther, T.; Krujatz, F. Optimized Protocol for Microalgae DNA Staining with SYTO9/SYBR Green I, Based on Flow Cytometry and RSM Methodology: Experimental Design, Impacts and Validation. *Methods Protoc.* **2022**, *5*, 76. [CrossRef] [PubMed]

26. Taborda, T.; Moniz, P.; Reis, A.; da Silva, T.L. Evaluating Low-Cost Substrates for Crypthecodinium Cohnii Lipids and DHA Production, by Flow Cytometry. *J. Appl. Phycol.* **2021**, *33*, 263–274. [CrossRef]
27. Zhong, W.; Zhang, Z.; Luo, Y.; Qiao, W.; Xiao, M.; Zhang, M. Biogas Productivity by Co-Digesting Taihu Blue Algae with Corn Straw as an External Carbon Source. *Bioresour. Technol.* **2012**, *114*, 281–286. [CrossRef]
28. Hoebler, C.; Barry, J.L.; David, A.; Delort-Laval, J. Rapid Acid Hydrolysis of Plant Cell Wall Polysaccharides and Simplified Quantitative Determination of Their Neutral Monosaccharides by Gas-Liquid Chromatography. *J. Agric. Food Chem.* **1989**, *37*, 360–367. [CrossRef]
29. Dubois, M.; Gilles, K.A.; Hamilton, J.K.; Rebers, P.A.; Smith, F. Colorimetric Method for Determination of Sugars and Related Substances. *Anal. Chem.* **1956**, *28*, 350–356. [CrossRef]
30. Salim, S.; Gilissen, L.; Rinzema, A.; Vermuë, M.H.; Wijffels, R.H. Modeling Microalgal Flocculation and Sedimentation. *Bioresour. Technol.* **2013**, *144*, 602–607. [CrossRef] [PubMed]
31. Zetsche, E.-M.; Meysman, F.J.R. Dead or Alive? Viability Assessment of Micro- and Mesoplankton. *J. Plankton Res.* **2012**, *34*, 493–509. [CrossRef]
32. Reavie, E.D.; Cangelosi, A.A.; Allinger, L.E. Assessing Ballast Water Treatments: Evaluation of Viability Methods for Ambient Freshwater Microplankton Assemblages. *J. Great Lakes Res.* **2010**, *36*, 540–547. [CrossRef]
33. Dias, C.; Gouveia, L.; Santos, J.A.L.; Reis, A.; Lopes da Silva, T. Using Flow Cytometry to Monitor the Stress Response of Yeast and Microalgae Populations in Mixed Cultures Developed in Brewery Effluents. *J. Appl. Phycol.* **2020**, *32*, 3687–3701. [CrossRef]
34. Rioboo, C.; O'Connor, J.E.; Prado, R.; Herrero, C.; Cid, Á. Cell Proliferation Alterations in Chlorella Cells under Stress Conditions. *Aquat. Toxicol.* **2009**, *94*, 229–237. [CrossRef] [PubMed]
35. da Silva, T.L.; Santos, C.A.; Reis, A. Multi-Parameter Flow Cytometry as a Tool to Monitor Heterotrophic Microalgal Batch Fermentations for Oil Production towards Biodiesel. *Biotechnol. Bioprocess Eng.* **2009**, *14*, 330–337. [CrossRef]
36. Salgado, E.M.; Esteves, A.F.; Gonçalves, A.L.; Pires, J.C.M. Microalgal Cultures for the Remediation of Wastewaters with Different Nitrogen to Phosphorus Ratios: Process Modelling Using Artificial Neural Networks. *Environ. Res.* **2023**, *231*. [CrossRef]
37. Yan, X.; Shan, S.; Li, X.; Xu, Q.; Yan, X.; Ruan, R.; Cheng, P. Carbon and Energy Metabolism for the Mixotrophic Culture of Chlorella Vulgaris Using Sodium Acetate as a Carbon Source. *Front. Microbiol.* **2024**, *15*, 1436264. [CrossRef] [PubMed]
38. Javed, F.; Hassan, A.A.; Zuhair, S. Al Microalgae–Bacteria Consortia for the Treatment of Fat, Oil, and Grease Wastewater: Recent Progress, Interaction Mechanisms, and Application Prospects. *J. Hazard. Mater. Adv.* **2025**, *19*, 100797. [CrossRef]
39. Khoo, C.G.; Lam, M.K.; Lee, K.T. Pilot-Scale Semi-Continuous Cultivation Ofmicroalgae Chlorella Vulgaris in Bubble Column Photobioreactor (BC-PBR): Hydrodynamics and Gas-Liquid Mass Transfer Study. *Algal Res.* **2016**, *15*, 65–76. [CrossRef]
40. Wang, C.; Lan, C.Q. Effects of Shear Stress on Microalgae—A Review. *Biotechnol. Adv.* **2018**, *36*, 986–1002. [CrossRef]
41. Zhang, Q.; Guan, Y.; Zhang, Z.; Dong, S.; Yuan, T.; Ruan, Z.; Chen, M. Sustainable Microalgae Cultivation: A Comprehensive Review of Open and Enclosed Systems for Biofuel and High Value Compound Production. *E3S Web Conf.* **2024**, *577*. [CrossRef]
42. Mirón, A.S.; Camacho, F.G.; Gómez, A.C.; Grima, E.M.; Chisti, Y. Bubble-Column and Airlift Photobioreactors for Algal Culture. *AIChE J.* **2000**, *46*, 1872–1887. [CrossRef]
43. Assunção, J.; Malcata, F.X. Enclosed "Non-Conventional" Photobioreactors for Microalga Production: A Review. *Algal Res.* **2020**, *52*, 102107. [CrossRef]
44. Ritu, J.R.; Ambati, R.R.; Ravishankar, G.A.; Shahjahan, M.; Khan, S. Utilization of Astaxanthin from Microalgae and Carotenoid Rich Algal Biomass as a Feed Supplement in Aquaculture and Poultry Industry: An Overview. *J. Appl. Phycol.* **2023**, *35*, 145–171. [CrossRef]
45. Chioccioli, M.; Hankamer, B.; Ross, I.L. Flow Cytometry Pulse Width Data Enables Rapid and Sensitive Estimation of Biomass Dry Weight in the Microalgae Chlamydomonas Reinhardtii and Chlorella Vulgaris. *PLoS ONE* **2014**, *9*, e97269. [CrossRef] [PubMed]
46. Deepa, P.; Sowndhararajan, K.; Kim, S. A Review of the Harvesting Techniques of Microalgae. *Water* **2023**, *15*, 3074. [CrossRef]
47. de Morais, E.G.; Sampaio, I.C.F.; Gonzalez-Flo, E.; Ferrer, I.; Uggetti, E.; García, J. Microalgae Harvesting for Wastewater Treatment and Resources Recovery: A Review. *N. Biotechnol.* **2023**, *78*, 84–94. [CrossRef]
48. Rani, S.; Ojha, C.S.P. Chlorella Sorokiniana for Integrated Wastewater Treatment, Biomass Accumulation and Value-Added Product Estimation under Varying Photoperiod Regimes: A Comparative Study. *J. Water Process Eng.* **2021**, *39*, 101889. [CrossRef]
49. Spennati, E.; Casazza, A.A.; Converti, A.; Padula, M.P.; Dehghani, F.; Perego, P.; Valtchev, P. Winery Waste Valorisation as Microalgae Culture Medium: A Step Forward for Food Circular Economy. *Sep. Purif. Technol.* **2022**, *293*, 121088. [CrossRef]
50. Naseema Rasheed, R.; Pourbakhtiar, A.; Mehdizadeh Allaf, M.; Baharlooeian, M.; Rafiei, N.; Alishah Aratboni, H.; Morones-Ramirez, J.R.; Winck, F.V. Microalgal Co-Cultivation -Recent Methods, Trends in Omic-Studies, Applications, and Future Challenges. *Front. Bioeng. Biotechnol.* **2023**, *11*, 1–25. [CrossRef]